

# The supporting information for Self-floating nanostructural Ni-NiO<sub>x</sub>/Ni foam for solar thermal water evaporation

Dandan Wu<sup>a</sup>, Dan Qu<sup>a\*</sup>, Wenshuai Jiang<sup>a</sup>, Ge Chen<sup>a</sup>, Li An<sup>a</sup>, Chunqiang Zhuang<sup>b</sup>

and Zaicheng Sun<sup>a</sup>

<sup>a</sup> Beijing Key Laboratory of Green Catalysis and Separation, Department of Chemistry and Chemical Engineering, College of Environmental and Energy Engineering, Beijing University of Technology, 100 Pingleyuan, Chaoyang District, Beijing 100124, P. R. China.

Email: [danqu@bjut.edu.cn](mailto:danqu@bjut.edu.cn) (DQ)

<sup>b</sup> Institute of Microstructure and Property of Advanced Materials, Beijing Key Lab of Microstructure and Property of Advanced Materials, Beijing University of Technology, Beijing 100124, China

# Content

---

| The supporting information | Page |
|----------------------------|------|
| <b>Figure S1</b>           | 3    |
| <b>Figure S2</b>           | 4    |
| <b>Figure S3-S4</b>        | 5    |
| <b>Figure S5-S6</b>        | 6    |
| <b>Figure S7</b>           | 7    |
| <b>The equation S1-S2</b>  | 8    |
| <b>Table S1-S2</b>         | 9    |
| <b>Figure S8</b>           | 10   |
| <b>Figure S9</b>           | 11   |
| <b>Table S3</b>            | 12   |
| <b>Figure S10</b>          | 13   |
| <b>Figure S11-S12</b>      | 14   |
| <b>Figure S13-S14</b>      | 15   |
| <b>Figure S15</b>          | 16   |
| <b>Table S4</b>            | 17   |
| <b>Reference</b>           | 18   |

---

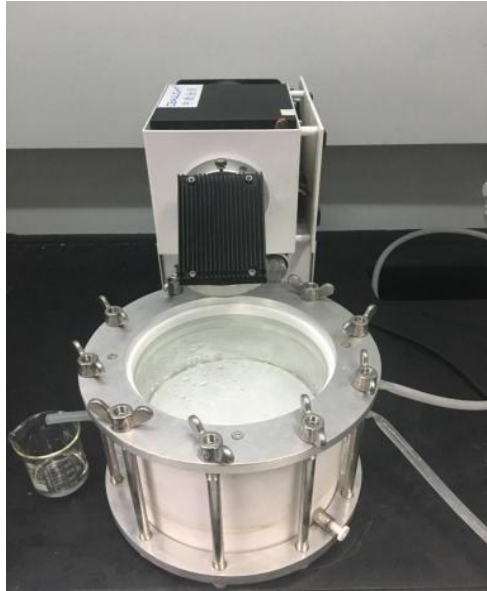


**Figure S1.** A home-made solar seawater desalination system to simulate solar seawater desalination.

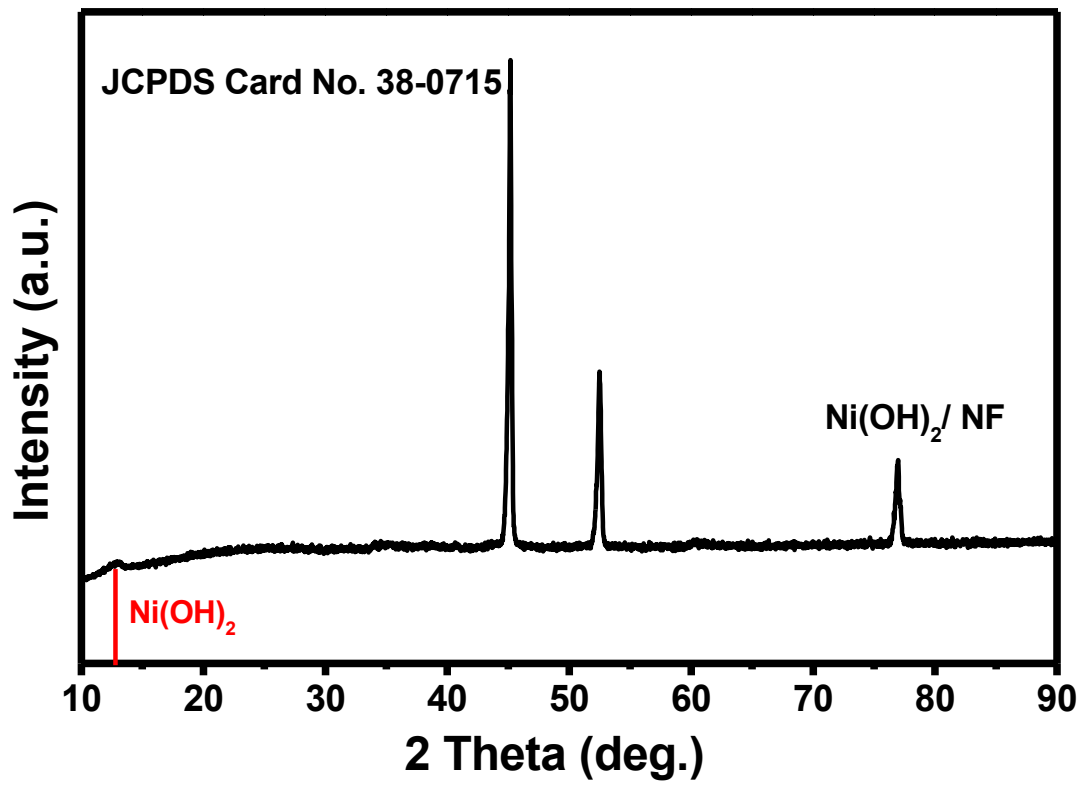


**Figure S2.** The X-ray diffraction (XRD) pattern of the Ni(OH)<sub>2</sub>/NF, JCPDS Card No.38-0715.

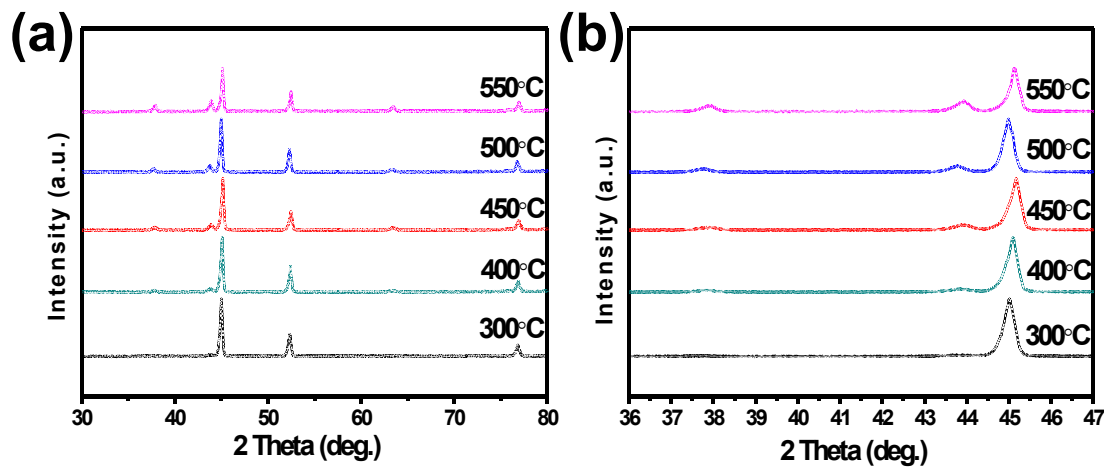


**Figure S3.** (a) The X-ray diffraction (XRD) pattern of the Ni(OH)<sub>2</sub> at different calcining temperatures from 300 to 500 °C for 1h. (b) Intensity variation diagram of characteristic peaks(43.3°) of NiO/NF.

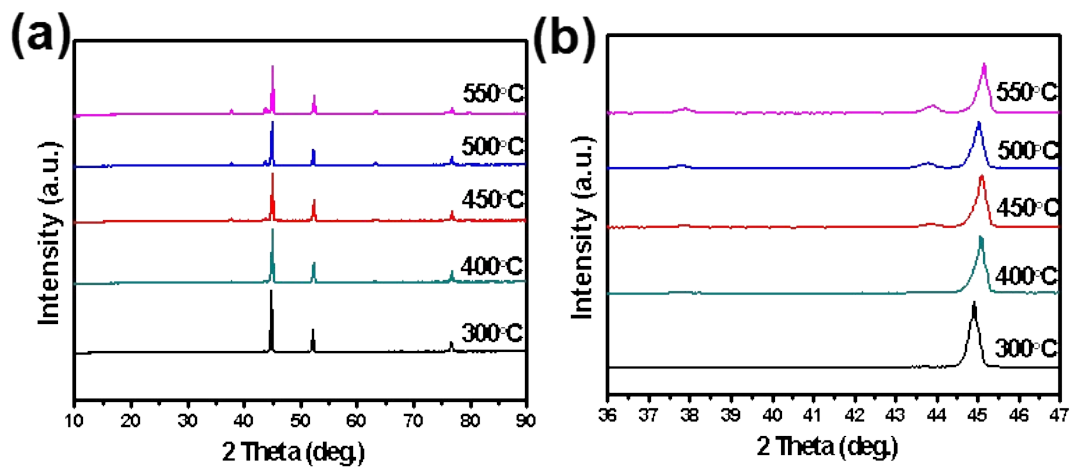


**Figure S4.** (a) The X-ray diffraction (XRD) pattern of NiO/NF at different temperature being reduced. (b) Intensity variation diagram of characteristic peak(43.3°) of NiO/NF.

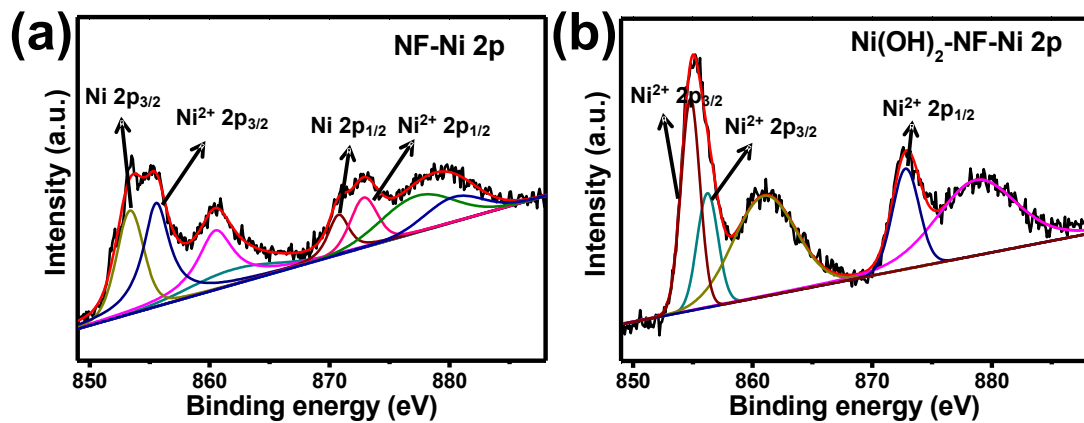


**Figure S5.** (a-b) The X-ray photoelectron spectroscopy (XPS) spectra of Ni foam,  $\text{Ni(OH)}_2$ .

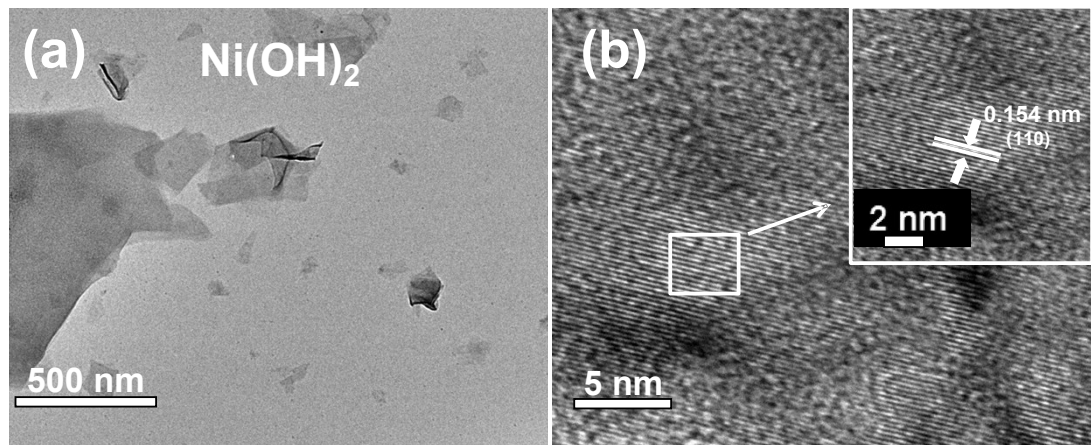


**Figure S6.** (a-b) The TEM and HRTEM of the  $\text{Ni(OH)}_2$ , the high resolution (HR) TEM image illustrates the lattice fringe space of 0.154 nm relating to the  $\text{Ni(OH)}_2$  (110).

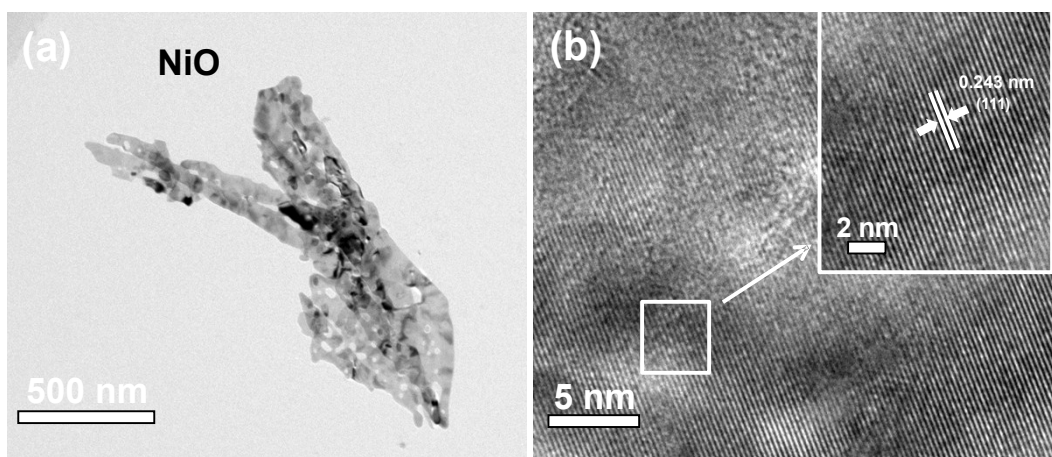


**Figure S7.** (a-b) The TEM and HRTEM of the  $\text{Ni}(\text{OH})_2$ , the high resolution (HR) TEM image illustrates the lattice fringe space of 0.243 nm relating to the  $\text{NiO}(111)$ .

### The equation S1

$$\alpha_{sol} = \frac{\int_{0.28\mu m}^{2.5\mu m} I_{sol} \cdot \alpha(\lambda) \cdot d\lambda}{\int_{0.28\mu m}^{2.5\mu m} I_{sol}(\lambda) \cdot d\lambda} = \frac{\int_{0.28\mu m}^{2.5\mu m} I_{sol}(\lambda) \cdot [1 - R(\lambda)] \cdot d\lambda}{\int_{0.28\mu m}^{2.5\mu m} I_{sol}(\lambda) \cdot d\lambda}$$

### The equation S2

$$\alpha(\lambda) = 1 - R(\lambda) - T(\lambda) = 1 - R(\lambda)$$

Where,  $\alpha_{sol}$  is overall solar absorptance.  $I_{sol}(l)$  is the radiation intensity at wavelength  $l$  in AM 1.5 solar spectrum .  $R(l)$ and  $T(l)$  are reflectance and transmittance at wavelength  $l$ , respectively.

**Table S1.** Calculation data of absorbance of different samples.

| Sample                       | Total(A,%) |
|------------------------------|------------|
| Ni foam                      | 68.09      |
| Ni(OH) <sub>2</sub> /Ni foam | 70.50      |
| NiO/Ni foam                  | 88.16      |
| Ni-NiO <sub>x</sub> /Ni foam | 90.31      |

**Table S2.** Calculation data of the thermal conductivity of different samples.

Thermal conductivity = thermal diffusion coefficient \* density \* specific heat.

| Sample                  | Temp.<br>°C | Dia.<br>mm | THK<br>mm | Volume<br>mm <sup>3</sup> | Mass<br>mg | Density<br>g/cm <sup>3</sup> | Thermal<br>diffusion<br>cm <sup>2</sup> /s | Specific<br>heat<br>J/g°C | Thermal<br>conductivity<br>(W/MK) |
|-------------------------|-------------|------------|-----------|---------------------------|------------|------------------------------|--|---------------------------|-----------------------------------|
| Ni foam                 | 30          | 12.7       | 0.293     | 37.10                     | 206.02     | 5.55                         | 0.0044                                     | 0.43                      | 1.04                              |
| Ni(OH) <sub>2</sub> /NF | 31          | 12.7       | 0.157     | 19.88                     | 92.99      | 4.68                         | 0.0033                                     | 0.45                      | 0.69                              |
| NiO/NF                  | 29          | 12.7       | 0.281     | 35.58                     | 172.75     | 4.86                         | 0.0047                                     | 0.43                      | 0.99                              |
| Ni-NiO <sub>x</sub> /NF | 30          | 12.7       | 0.266     | 33.68                     | 158.98     | 4.72                         | 0.0012                                     | 0.43                      | 0.24                              |

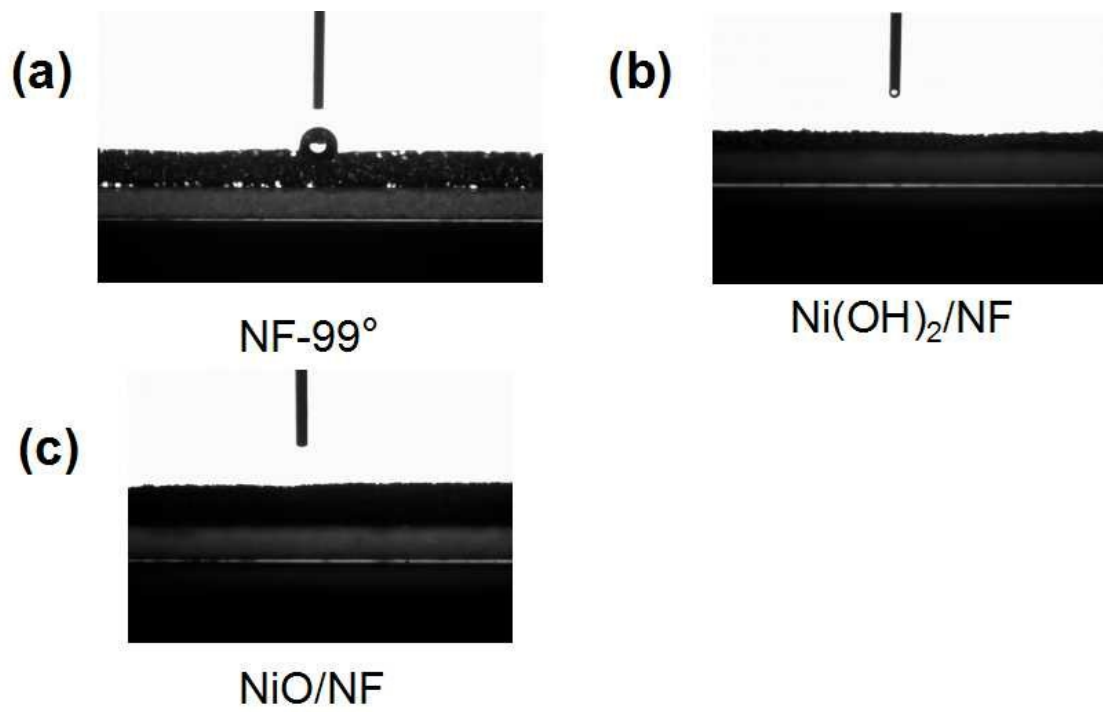


**Figure S8.** (a-c) The contact angles of the original Ni foam, Ni(OH)<sub>2</sub> nanosheets, NiO nanosheets samples display super hydrophilic behavior.

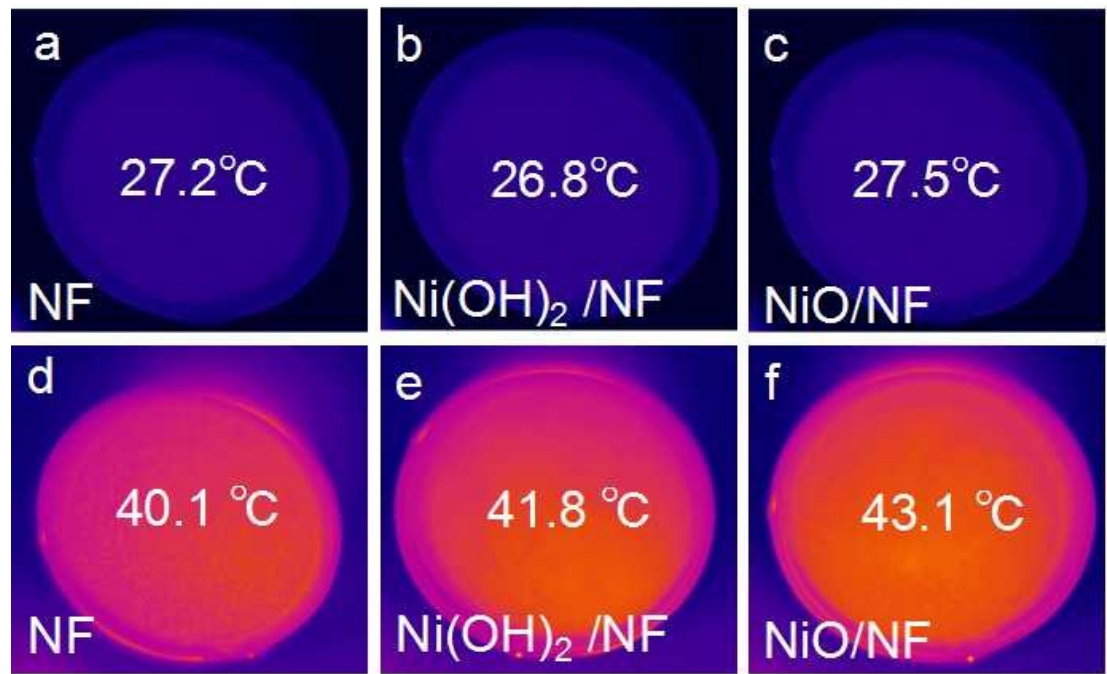


**Figure S9.** (a-f) The infrared images of water and NF, Ni(OH)<sub>2</sub>/NF and NiO/NF films floating on the water before and after 2 hours irradiation.

**Table S3.** Calculation data of the evaporation rate and conversion efficiency of different samples.

| Film                         | Fitting equation | Evaporation rate<br>of water(v,kg/m <sup>2</sup> h) | Power of the<br>evaporation<br>(kJ/m <sup>2</sup> h) | Conversion<br>efficiency(η,%) |
|------------------------------|------------------|---|--|-------------------------------|
| Darkness                     | Y=0.0566x+8E-05  | 0.0566  | 2444.60  | 3.84                          |
| Water without light          | Y=0.1545x+0.0123 | 0.1545  | 2439.35  | 10.47                         |
| Water under light            | Y=0.6941x-0.1019 | 0.6941  | 2426.40  | 46.78                         |
| Ni foam                      | Y=0.9683X-0.0451 | 0.9683  | 2412.54  | 64.89                         |
| Ni(OH) <sub>2</sub> /Ni foam | Y=1.1674x-0.0963 | 1.1674  | 2409.39  | 78.13                         |
| NiO/Ni foam                  | Y=1.302x-0.1257  | 1.302   | 2406.99  | 87.05                         |
| Ni-NiO <sub>x</sub> /Ni foam | Y=1.4092x-0.1303 | 1.4092  | 2398.38  | 93.88                         |

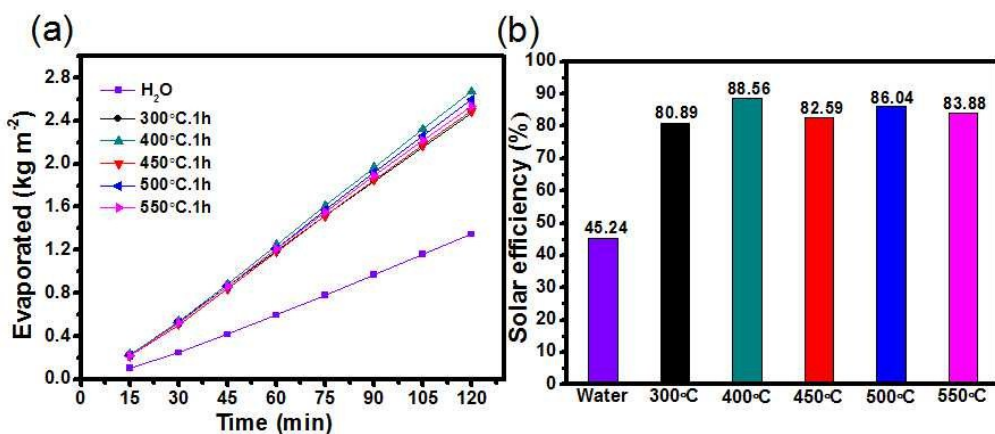


**Figure S10.** (a) The step 2 of the synthesis process (optimize preparation condition 1) : the dependence of evaporation rate of water on irradiation time for the different calcination temperature of  $\text{Ni(OH)}_2/\text{NF}$  samples under 1 sun simulated light ( $100 \text{ mW cm}^2$ ). The evaporation of water makes a blank contrast. (b) Corresponding solar efficiency of the above 6 samples.

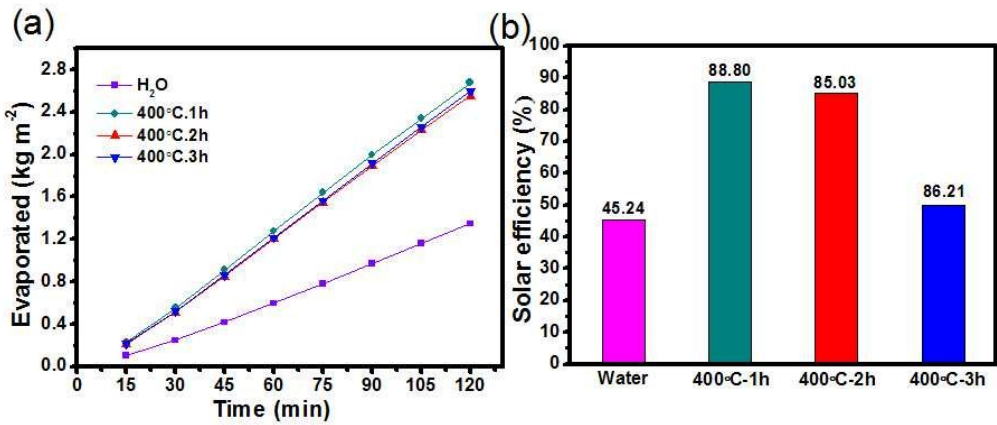


**Figure S11.** (a) The step 2 of the synthesis process (optimize preparation condition 2) : the dependence of evaporation rate of water on irradiation time for the different calcination time of Ni(OH)<sub>2</sub>/NF samples under 1 sun simulated light (100 mW cm<sup>2</sup>). The evaporation of water makes a blank contrast. (b) Corresponding solar efficiency of the above 4 samples.

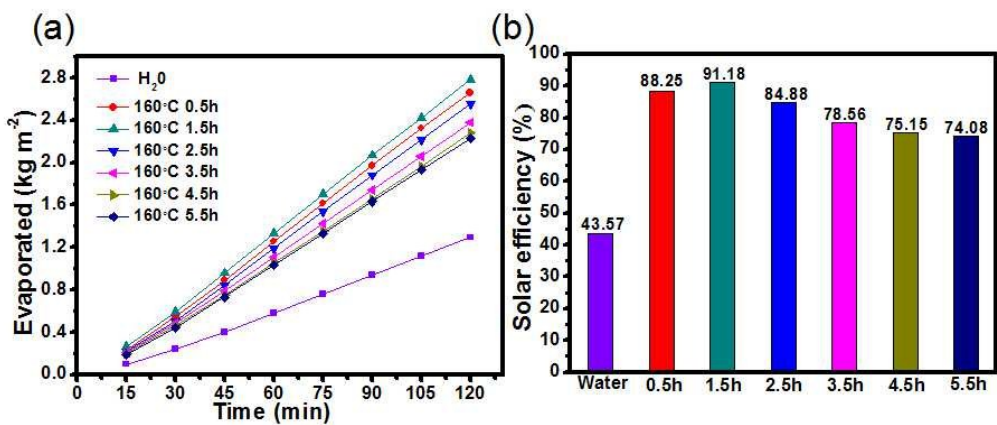


**Figure S12.** (a) The step 3 of the synthesis process (optimize preparation condition 3) : the dependence of evaporation rate of water on irradiation time for the different reduction time of NiO/NF samples under 1 sun simulated light (100 mW cm<sup>2</sup>). The evaporation of water makes a blank contrast. (b) Corresponding solar efficiency of the above 7 samples.

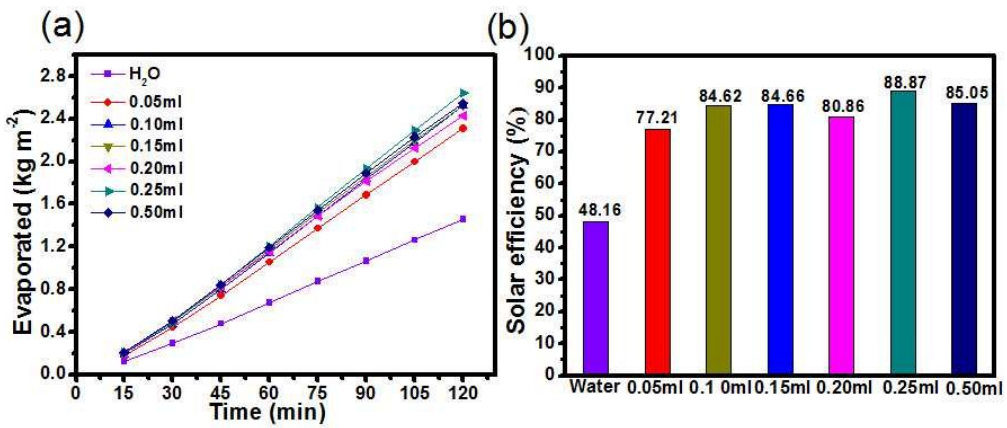


**Figure S13.** (a) The step 3 (Optimize preparation condition 4): the dependence of evaporation rate of water on irradiation time for the different reduction concentration of NiO/NF samples under 1 sun simulated light ( $100 \text{ mW cm}^2$ ). The evaporation of water makes a blank contrast. (b) Corresponding solar efficiency of the above 7 samples.

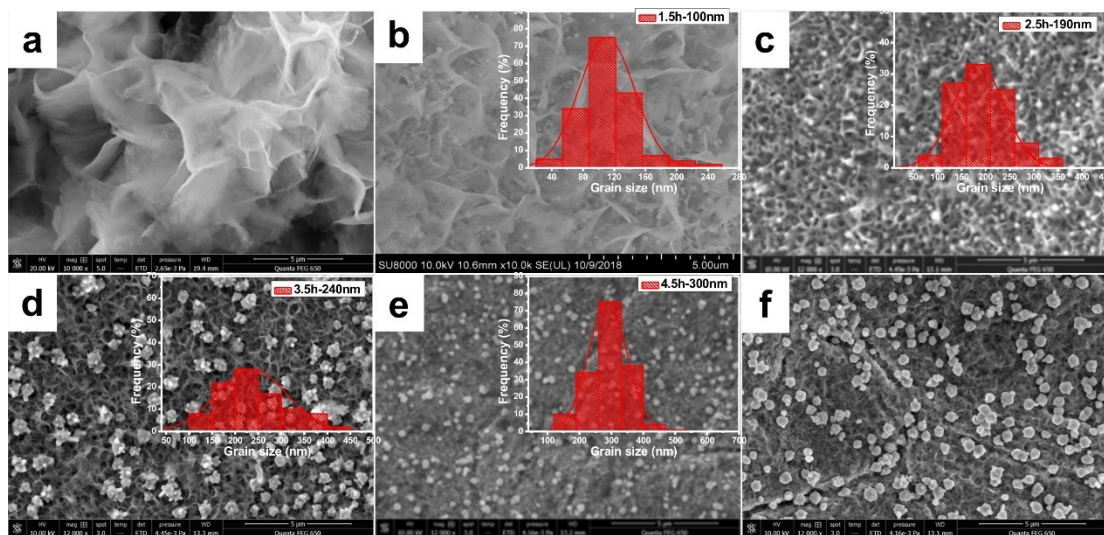


**Figure S14.** (a-f) SEM images of the different reduction time (0.5 h-5.5 h) of NiO/NF Samples.

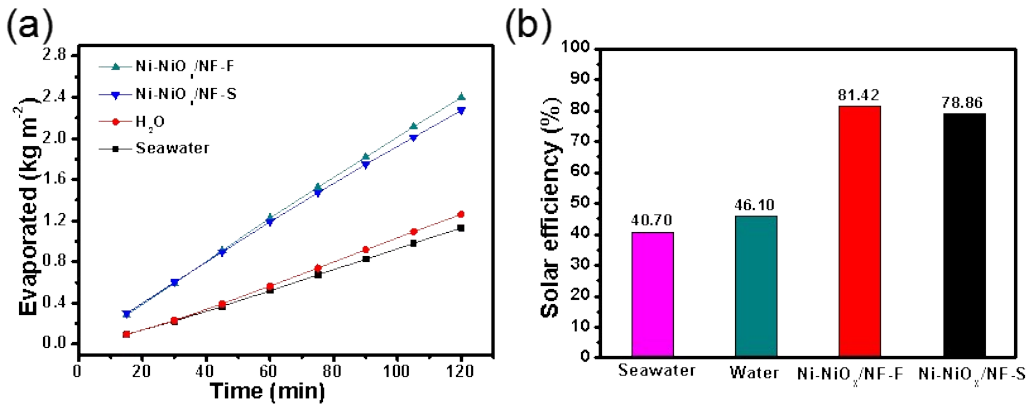


**Figure S15.** (a) The evaporation rate curve of seawater, H<sub>2</sub>O, Ni-NiO<sub>x</sub>/NF-S(seawater), Ni-NiO<sub>x</sub>/NF-F(fresh water). (All experiments were conducted in ambient temperature of 15-18°C with a humidity of 18-20%), (b) the photothermal conversion efficiency of the seawater, H<sub>2</sub>O, Ni-NiO<sub>x</sub>/NF-S(seawater), Ni-NiO<sub>x</sub>/NF-F(fresh water). Due to the room temperature for this measurement is lower than that for Figure S10-13 (RT=25-27°C). The environmental temperature is a critical factor for the water evaporation. The quantity of heat is same from the solar thermal conversion, the temperature change is the same according to the equation ( $Q = mC_p\Delta T$ ). Suppose that the Q keeps constant for the one sample, then  $\Delta T$  should not change. That indicates the temperature of water surface will increase from 15 to 25°C in this case. In the case of Figure S10, the temperature will turn to 35 °C. But the water evaporation rate will slower at 25 °C than that at 35°C . That's why the water evaporation rate decreases.

**Table S4** The comparison of photothermal evaporation performance of Ni-NiO<sub>x</sub>/NF and the reported related photothermal materials

| Sample  | Light intensity (kw·m <sup>-2</sup> ) | Water evaporation rate (v,kg·m <sup>-2</sup> ·h <sup>-1</sup> ) | Conversion Efficiency (η,%) | Classification of solar thermal materials | Reference  |
|---|---------------------------------------|---|-----------------------------|---|--|
| Al NP/AAM   | 1                                     | 0.92  | 58%                         | Metallic plasmonic material               | <i>Nat. Photonics</i> S1 <sup>1</sup>                |
| Au film/Airlaid paper   | 4.5                                   | 5.5   | 77%                         | Metallic plasmonic material               | <i>Adv. Mater.</i> S2 <sup>2</sup>                   |
| Black gold membrânes  | 1                                     | 0.68  | 42.5%                       | Metallic plasmonic material               | <i>Nat. Commun.</i> S3 <sup>3</sup>                  |
| TiO <sub>2</sub> /Au NP film/AAO                              | 1                                     | --  | --                          | Metallic plasmonic material               | <i>ACS Appl. Mater. Interfaces</i> S4 <sup>4</sup>   |
| Au/D-NPT/AAO  | 4                                     | ~5.2  | 90%                         | Metallic plasmonic material               | <i>Sci. Adv.</i> S5 <sup>5</sup>                     |
| Black Al-Ti-O membrane  | 1                                     | 1.23  | 77.5%                       | Metallic plasmonic material               | <i>Nano Energy</i> S6 <sup>6</sup>                   |
| <b>Ni-NiO<sub>x</sub>/NF</b>                                  | <b>1</b>                              | <b>1.41</b>   | <b>93.9</b>                 | Metallic plasmonic material               | <b>This work</b>                                     |
| rGO/MWCNT   | 1                                     | 1.22  | 80.3%                       | Carbon-based material                     | <i>J. Mater. Chem. A</i> S7 <sup>7</sup>             |
| Carbon foam/Exfoliated graphite                               | 1                                     | 1.02  | 64%                         | Carbon-based material                     | <i>Nat. Commun.</i> S8 <sup>8</sup>                  |
| Hierarchical graphene foam                                    | 1                                     | 1.46  | >90%                        | Carbon-based material                     | <i>Adv. Mater.</i> S9 <sup>9</sup>                   |
| RGO+bacterial nanocellulose aerogel                           | 10                                    | 11.8  | 83%                         | Carbon-based material                     | <i>Adv. Mater.</i> S10 <sup>10</sup>                 |
| 3D-CG/GN  | 1                                     | 1.25  | 85.6%                       | Carbon-based material                     | <i>Adv. Mater.</i> S11 <sup>11</sup>                 |
| Black TiOx  | 1                                     | 0.8012  | 50.30%                      | Semiconductor material                    | <i>Adv. Energy Mater.</i> S12 <sup>12</sup>          |
| Black Titania nanocage  | 1                                     | 1.13  | 70.9%                       | Semiconductor material                    | <i>ACS Appl. Mater. Interfaces</i> S13 <sup>13</sup> |
| Cu <sub>7</sub> S <sub>4</sub> nanocrystal film               | 1.006<br>(Infrared lamp)              | --  | 77.10%                      | Semiconductor material                    | <i>Small</i> S14 <sup>14</sup>                       |
| Ti <sub>2</sub> O <sub>3</sub> NP/Cellulose membrane          | 1                                     | 1.32  | 83%                         | Semiconductor material                    | <i>Adv. Mater.</i> S16 <sup>15</sup>                 |
| PPy/Coated SS   | 1                                     | 0.92  | 58%                         | Organic material                          | <i>Adv. Mater.</i> S17 <sup>16</sup>                 |
| Bubble wrap/commercial spectrally selective coating on copper | 1                                     | --  | 64%                         | Composite material                        | <i>Nat. Energy</i> S17 <sup>17</sup>                 |

## Reference

1. L. Zhou, Y. Tan, J. Wang, W. Xu, Y. Yuan, W. Cai, S. Zhu and J. Zhu, *Nat. Photonics*, 2016, **10**, 393.
2. Y. Liu, S. Yu, R. Feng, A. Bernard, Y. Liu, Y. Zhang, H. Duan, W. Shang, P. Tao, C. Song and T. Deng, *Adv. Mater.*, 2015, **27**, 2768-2774.
3. K. Bae, G. Kang, S. K. Cho, W. Park, K. Kim and W. J. Padilla, *Nat. Commun.*, 2015, **6**, 10103.
4. Y. Liu, J. Lou, M. Ni, C. Song, J. Wu, N. P. Dasgupta, P. Tao, W. Shang and T. Deng, *ACS Appl. Mater. Interfaces*, 2016, **8**, 772-779.
5. L. Zhou, Y. Tan, D. Ji, B. Zhu, P. Zhang, J. Xu, Q. Gan, Z. Yu and J. Zhu, *Sci. Adv.*, 2016, **2**, e1501227.
6. L. Yi, S. Ci, S. Luo, P. Shao, Y. Hou and Z. Wen, *Nano Energy*, 2017, **41**, 600-608.
7. Y. Wang, C. Wang, X. Song, S. K. Megarajan and H. Jiang, *J. Mater. Chem. A.*, 2018, **6**, 963-971.
8. H. Ghasemi, G. Ni, A. M. Marconnet, J. Loomis, S. Yerci, N. Miljkovic and G. Chen, *Nat. Commun.*, 2014, **5**, 4449.
9. H. Ren, M. Tang, B. Guan, K. Wang, J. Yang, F. Wang, M. Wang, J. Shan, Z. Chen, D. Wei, H. Peng and Z. Liu, *Adv. Mater.*, 2017, **29**, 1702590.
10. Q. Jiang, L. Tian, K.-K. Liu, S. Tadepalli, R. Raliya, P. Biswas, R. R. Naik and S. Singamaneni, *Adv. Mater.*, 2016, **28**, 9400-9407.
11. Y. Li, T. Gao, Z. Yang, C. Chen, W. Luo, J. Song, E. Hitz, C. Jia, Y. Zhou, B. Liu, B. Yang and L. Hu, *Adv Mater.*, 2017, **29**, 1700981.
12. M. Ye, J. Jia, Z. Wu, C. Qian, R. Chen, P. G. O'Brien, W. Sun, Y. Dong and G. A. Ozin, *Adv. Energy Mater.*, 2017, **7**, 1601811.
13. G. Zhu, J. Xu, W. Zhao and F. Huang, *ACS Appl. Mater. Interfaces*, 2016, **8**, 31716-31721.
14. C. Zhang, C. Yan, Z. Xue, W. Yu, Y. Xie and T. Wang, *Small*, 2016, **12**, 5320-5328.
15. J. Wang, Y. Li, L. Deng, N. Wei, Y. Weng, S. Dong, D. Qi, J. Qiu, X. Chen and T. Wu, *Adv. Mater.*, 2017, **29**, 1603730.
16. L. Zhang, B. Tang, J. Wu, R. Li and P. Wang, *Adv. Mater.*, 2015, **27**, 4889-4894.
17. G. Ni, G. Li, Svetlana V. Boriskina, H. Li, W. Yang, T. Zhang and G. Chen, *Nat. Energy*, 2016, **1**, 16126.